Available online at www.sciencedirect.com
SCIENCE DIRECT
Polymer 46 (2005) 3831–3837
polymer
www.elsevier.com/locate/polymer

A unique crystallization and double melting behavior of a polyimide derived from 3,3′,4,4′-biphenyltetracarboxylic dianhydride and 1,4-bis(3-aminopropyl)piperazine

Naiheng Song, Dianjun Yao, Zhi Yuan Wang*, Pudupadi R. Sundararajan*

Department of Chemistry, Carleton University, 1125 Colonel By Drive, Ottawa, Ont., Canada K1S 5B6

Received 3 February 2005; received in revised form 6 March 2005; accepted 8 March 2005
Available online 2 April 2005

Abstract

A unique crystallization and melting behavior of a novel semicrystalline polyimide derived from 3,3′,4,4′-biphenyltetracarboxylic dianhydride and 1,4-bis(3-aminopropyl)piperazine were studied by differential scanning calorimetry (DSC) with and without temperature modulation and wide-angle X-ray diffraction (WAXD). Polymer samples isolated from a chloroform solution showed melting transitions in the DSC. However, WAXD traces showed crystallinity only after annealing above the glass transition, for about 2 h. For samples crystallized from the melt, crystallization could be achieved only in a narrow crystallization range of 200–220 °C, after 10 h. A maximum crystallinity of this polyimide was found to be 30%. Two distinct melting transitions were observed by DSC, which could be explained using a partial disordering—reorganization—final melting model.

Keywords: Crystallization; Melting; Semicrystalline polyimide

1. Introduction

The development of polymeric materials suitable for multi-purpose technological applications requires an ability to manipulate the morphological features of a given polymer to render the desired functional properties. Semicrystalline polymers are well suited in this regard due to their varied morphological attributes and structural tunability. Several semicrystalline polymer systems are known, such as polystyrenes [1], polyethers [2], polyesters [3], and polypropylenes [4]. The morphologies of these polymers can be controlled by various means to achieve properties such as optical clarity and mechanical strength.

Polyimides are high-performance polymers that have applications ranging from aerospace to microelectronics [5,6]. Improvement of the polyimide properties has mainly relied on synthesizing new polymers and physical blending [7]. Although the rigid backbone structures are known to be capable of stacking to form layered structures, only a few aromatic polyimides are known to be semicrystalline [8]. Introduction of aliphatic chain segments and flexible linkages such as an ester into the polyimide backbone can induce order in polyimides, as has been shown in most cases for liquid crystalline polyimides [9].

Since polyimides are widely used as thin films or coatings in devices, their properties can also be changed by supramolecular assembly or forming a multilayer film from different materials. Recently, a simple and fast multilayer assembling method based on spin-coating technique was reported by us [10]. A series of polyimides containing basic piperazine units in the backbone were used in pair with an acid polyimide to form multilayer films on substrates. For example, by alternately spin-coating the title polymer (BPAPP, Fig. 1) in chloroform and the acid polyimide in tetrahydrofuran, a multilayer build-up was achieved and the thickness of each single layer could be easily controlled down to 2 nm. The multilayer film thus fabricated with 12 bi-layers of BPAPP/acid polyimide was found to be uniform and transparent. However, thick films (e.g. >2 μm) cast from a solution of BPAPP in chloroform appeared opaque and showed birefringence under the polarizing microscope.

* Corresponding authors. Tel.: +1 613 5202600x2713; fax: +1 613 5202316.
E-mail address: wangw@ccs.carleton.ca (Z.Y. Wang).

0032-3861/$ - see front matter © 2005 Elsevier Ltd. All rights reserved.
doi:10.1016/j.polymer.2005.03.024

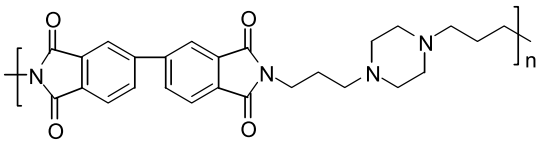

Fig. 1. Chemical structure of BPAPP.

Given that the crystalline morphology of ultrathin films (e.g. <100 nm) may change greatly with the film thickness [11], BPAPP is quite attractive for fabricating multilayer films that have interlayers whose crystallinity and morphology are tunable by controlling the deposition thickness or external stimuli (e.g. heat treatment). Therefore, it would be interesting and useful to study the crystallization behavior of BPAPP in the bulk. Such a study on the crystallization and morphology of this polymer would help in our understanding of the role of acid–base interactions on the morphology in multi-layered films. This is similar to the role of self-assembly in the formation of tertiary structures. In this paper, we describe (i) the unique solubility of BPAPP, (ii) the effect of annealing on the crystallization of samples precipitated from chloroform and acetone, and (iii) the difference between annealing the solution cast film and crystallization from the melt. The double melting behavior is also discussed.

2. Experimental

The polyimide BPAPP was synthesized through the polycondensation reaction of 3,3′,4,4′-biphenyltetracarboxylic dianhydride and 1,4-bis(3-aminopropyl)piperazine in boiling acetic acid [10]. Although the acid–base interaction between BPAPP and organic acid was present, BPAPP contained no acetic acid when the polymer was obtained by precipitation of the reaction solution into aqueous potassium carbonate solution, as evident from the ^{1}H NMR and IR spectroscopies [10]. BPAPP has a T_g of 148 °C.

Inherent viscosities of BPAPP in acetic acid and in chloroform were measured with an Ubbelohde capillary viscometer at 30.0 ± 0.1 °C with a concentration of 0.5 g/dL. Both the standard differential scanning calorimetry (DSC) and temperature modulated DSC (TMDSC) analyses were carried out in nitrogen on a TA DSC Q100. A typical TMDSC experiment was run with a heating rate of 3 °C/min, a modulation amplitude of 1 °C, and a modulation period of 1 min. Isothermal annealing and crystallization of polymer samples for DSC analysis were carried out directly in the DSC instrument under a nitrogen atmosphere. Isothermal annealing of polymer films for X-ray diffraction was performed in a heating box under argon. The films were prepared by casting a solution of BPAPP in chloroform (ca. 10 w/v%) onto glass slides and had a thickness in the range of 8–15 μm. The thickness of films was determined by using a Metricon 2010 prism coupler. X-ray powder diffraction patterns were recorded by using a Phillips PW1730 diffractometer with Cu K_α source ($\lambda=0.154$ nm). The Jade 5 XRD Pattern Processing software (Materials Data Inc.) was used for analysis of the diffraction patterns. Small-angle laser light scattering (SALS) patterns were recorded on polaroid land films in the H_v mode using a set-up equipped with a 10 mV He–Ne laser with $\lambda=0.6328$ μm, a rotatable analyzer.

3. Results and discussion

3.1. Solubility

The polyimide BPAPP exhibited a unique solubility, as it was readily soluble in organic acids (e.g. acetic acid) and only in chloroform and dichloromethane (Table 1). The commonly used polar solvents for polyimides, such as *N*,*N*-dimethylacetamide (DMAc), *m*-cresol and dimethylsulfoxide (DMSO), were non-solvents for BPAPP. Even the solvents that have the solubility parameter similar to chloroform, including chlorobenzene, 1,1,2-trichloroethane, tetrahydrofuran and cyclohexanone, were found to be incapable of even swelling this polymer. The high solubility of BPAPP in acetic acid can be easily understood in terms of the acid–base interaction, but the unique solubility in chloroform and in dichloromethane cannot be explained by simple solubility parameter criterion. The individual δ factors of various solvents (i.e. the dispersion term, polarity term and the hydrogen-bond term) as well as their molecular sizes in terms of their molar volumes are compared in Table 1. However, none of them can be used to account for the solubility of BPAPP in only chloroform and dichloromethane.

A possible explanation may come from the hydrogen-bond formation between BPAPP and the chlorinated alkanes as a hydrogen donor. Several studies [12] support this conclusion. Desiraju and Steiner [12a] gave a number of examples of crystal structures involving hydrogen bonds to the C–Cl group. A self-assembly process driven by ‘halogen bonding’ was discussed by Corradi et al. [12b] Abraham et al. [12c] compared the hydrogen bond basicities of several choloroalkanes and found hexachlorocyclohexanes as a strong hydrogen bond base. The crystal structure of a Ru complexed amine was found to involve chloroform and water stabilizing the structure through hydrogen bonds [12d]. In a study of benzoic acids, amines and naphthols in chloroform, Majumdar et al. [12e] suggested charge transfer and other weak interactions. Thus, the solubility of BPAPP in chloroform and dichloromethane can be attributed to such ‘halogen bonding’ interactions. The inherent viscosities of BPAPP in acetic acid and chloroform (measured with a concentration of 0.5 dL/g) were 0.67 and 0.33 dL/g, respectively. The higher inherent viscosity in acetic acid

Table 1
Solubility of BPAPP in various organic solvents

Solvents	Solubility	Solubility parameter[a] (δ)	Dispersive term[a] (δ_D)	Polar term[a] (δ_P)	Hydrogen bonding[a] (δ_H)	Molar volume[a] (cm^3/mol)
Chloroform	+	19.0	17.8	3.1	5.7	80.7
Chlorobenzene	−	19.6	19.0	4.3	2.0	102.1
Cyclohexanone	−	19.6	17.8	6.3	5.1	104.0
Acetone	−	20.1	15.5	10.4	7.0	74.0
Dichloromethane	+	20.3	18.2	6.3	6.1	63.9
Acetic acid	+	21.3	14.5	8.0	13.5	57.1
m-Cresol	−	22.7	18.0	5.1	12.9	104.7
DMF	−	24.8	17.4	13.7	11.3	77.0
DMSO	−	26.6	18.4	16.4	10.2	71.3

Note: '+' = soluble; '−' = insoluble. NA = not available.
[a] From J. Brandrup and E. H. Immergut, Polymer Handbook 3rd ed, Wiley; 1989.

indicates a more extended conformation of the polymer compared to that in chloroform.

3.2. Solvent-dependent crystallization

BPAPP isolated from its acetic acid solution showed no melting transition in DSC heating scans. The films cast from the acetic acid solution were highly transparent. However, when the polymer was re-dissolved in chloroform and precipitated from methanol, two endothermic transitions were seen at ~165 and 260 °C in the first heating scan (Fig. 2). The films cast from the chloroform solution and dried at 80 °C under vacuum appeared opaque and showed birefringence under a polarized microscope and the same double-melting transitions on the first DSC heating scan. However, the WAXD revealed no distinct crystalline diffraction (scan a, Fig. 3). Thus, chloroform appears to be quite unique for BPAPP since it can induce the polymer crystallization to a certain degree in the precipitated and solution-cast samples, as seen from the melting transitions in the DSC traces. It is likely that the crystallites are too small to be resolved with X-ray diffraction. Upon quenching from the melt, it is seen that the melting endotherms are absent in the second scan (trace b, Fig. 2). The broad exotherm centered about 200 °C here (and in Fig. 7(B), curve a) is attributed to the overshoot resulting from mechanical relaxation of the glass.

3.3. Thermal crystallization

When the polymer samples isolated from acetic acid and those from chloroform were heated to a temperature above the second endothermic transition (to 300 °C) and quenched, the second scan in the DSC analysis showed no melting transition (e.g. trace b, Fig. 2). The slow heating and cooling of the samples at a rate of 2 or 5 °C/min or isothermal annealing for 10 h at 180 or 240 °C could not recover the endothermic transitions. However, when these samples were melted at 300 °C and were isothermally crystallized for 10 h within a temperature range of 200–220 °C, the two melting transitions reappeared on the DSC heating scan with the first melting transition shifted to higher temperatures (traces a and c, Fig. 4). This specific, narrow temperature range for melt quenched BPAPP to crystallize may be attributed to the sparcity of nucleation

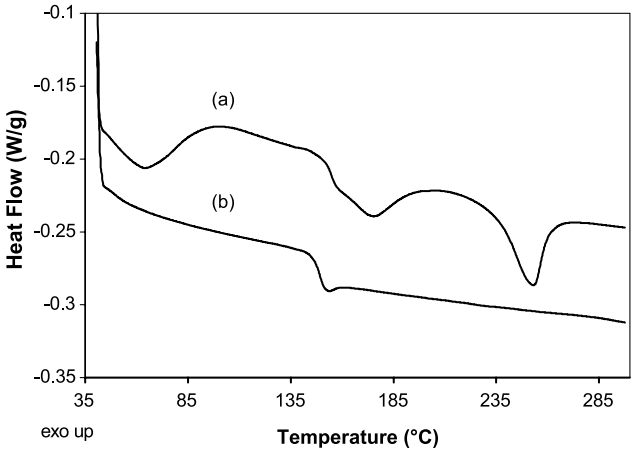

Fig. 2. DSC traces (in nitrogen flow) of BPAPP isolated from chloroform with a heating rate of 10 °C/min: (a) the first heating and (b) the second heating.

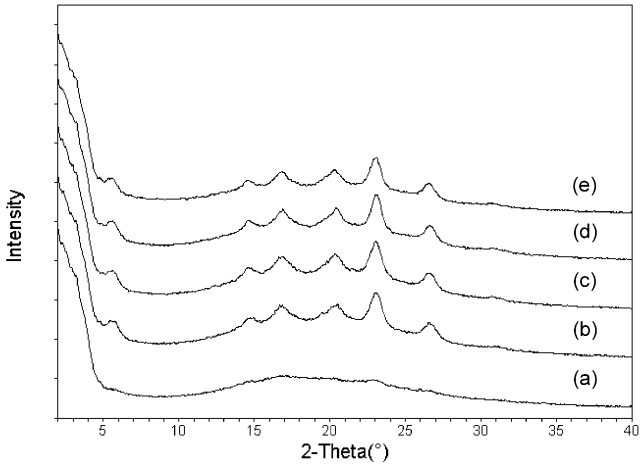

Fig. 3. Wide-angle X-ray diffraction of BPAPP films that were annealed (in nitrogen flow) for 2 h at (a) 80 °C, (b) 180 °C, (c) 200 °C, (d) 220 °C and (e) 245 °C.

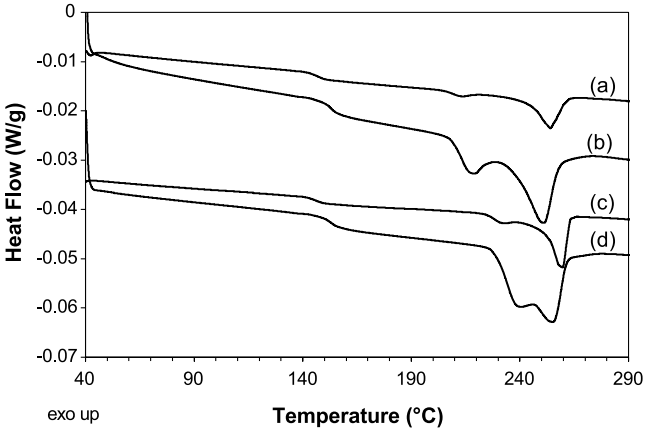

Fig. 4. DSC traces of BPAPP with different thermal histories (in nitrogen flow) with a heating rate of 3 °C/min. Traces (a) and (c) are from BPAPP samples that were heated to 300 °C, and crystallized for 10 h at 200 and 220 °C, respectively; traces (b) and (d) are from BPAPP samples that were isolated from chloroform and were annealed for 2 h at 200 and 220 °C, respectively. The heat flows are normalized to the sample weight.

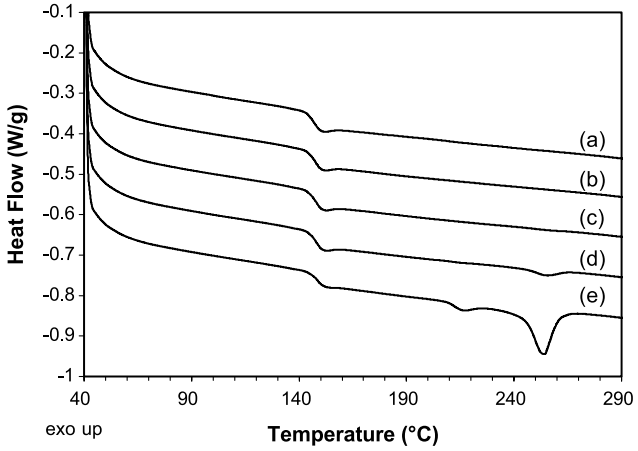

Fig. 5. DSC traces of BPAPP (in nitrogen flow) with a heating rate of 10 °C/min. The BPAPP samples were pre-heated to 300 °C, and crystallized at 200 °C for (a) 10 min, (b) 30 min, (c) 1 h, (d) 2 h, and (e) 5 h.

and growth at temperatures less than or higher than the regime of 200–220 °C. This crystallization range is half way between the T_m and T_g of 260 and 148 °C, respectively, which would correspond to the maximum crystal growth.

With the samples isolated from chloroform (i.e. not quenched from 300 °C), a much shorter annealing time of 2 h (at 200 and 220 °C) was sufficient to induce crystallinity. The DSC traces for this case are also shown in Fig. 4 (traces c and d for samples annealed at 200 and 220 °C, respectively). Thus, annealing induced crystallization of BPAPP seems to occur more readily with the samples precipitated from chloroform, than with samples crystallized from the melt. Although the two exhibited basically the same double-melting pattern on DSC, they are quite different in terms of heat of fusion. For example, BPAPP thermally crystallized at 200 °C for 10 h had a total heat of fusion (ΔH_{1+2}) of 10.1 J/g, while BPAPP precipitated from its chloroform solution and annealed at 200 °C for 2 h was found to have a much larger ΔH_{1+2} of 17.8 J/g. In addition, the contribution of the heat of fusion of the low temperature endotherms (ΔH_1) to ΔH_{1+2} was different between the thermally crystallized from the melt and chloroform-precipitated samples. The former has a $\Delta H_1/\Delta H_{1+2}$ value of ~0.1 and the latter ~0.3. Fig. 5 shows the DSC thermograms recorded for the samples that were melt-crystallized for various times at 200 °C. While no endotherm was observed with short crystallization times (traces a–c, in Fig. 5), it took 2 h at 200 °C to detect a small endotherm at around 257 °C (trace d, Fig. 5). A clear double-melting pattern was developed after annealing for 5 h (trace e, Fig. 5). However, the ΔH_{1+2} (4.89 J/g) is still less than one third of the sample isolated from chloroform and annealed at 200 °C for 2 h. Therefore, both slow nucleation and slow crystal growth are indicated in the thermal crystallization from the melt. For the samples precipitated from chloroform and annnealed at 200 °C for 2 h, the SALS patterns in the H_v mode showed the spherulite size to be about 20 μm.

3.4. Double-melting behavior

The temperature dependence of the two endothermic transitions of BPAPP was studied by the DSC analysis of polymer samples isolated from its chloroform solution and annealed for 2 h at different temperatures (160–245 °C) above the T_g but lower than the second transition (Fig. 6). With the increase in the annealing temperature, the first endothermic transition shifted to a higher temperature and closer to the second endothermic transition (traces a–d, Fig. 6). The two transitions coalesced at the annealing temperature of 245 °C to give a single sharp melting peak at 260 °C (trace e, Fig. 6).

To examine if the change in the first endotherm is due to

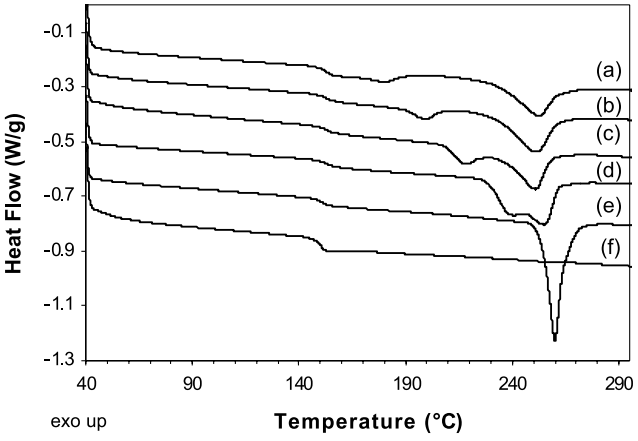

Fig. 6. Standard DSC traces (in nitrogen flow) of BPAPP isolated from chloroform, with a heating rate of 10 °C/min. The BPAPP samples were annealed prior to the DSC measurements for 2 h at (a) 160 °C, (b) 180 °C, (c) 200 °C, (d) 220 °C, (e) 245 °C, and (f) 270 °C. The heat flows are not normalized to the sample weight.

a polymorphic transition, BPAPP films (ca. 10 μm thick) were prepared by casting from chloroform solution, annealed for 2 h at different temperatures (180–245 °C) in nitrogen and diffraction patterns were recorded (Fig. 3). The WAXD showed six diffraction peaks for all the annealed films, with the *d*-spacings of 15.65, 6.02, 5.23, 4.33, 3.84 and 3.33 A (traces b–e, Fig. 3). The WAXD pattern did not change upon annealing at different temperatures, including the temperature at which the two endotherms coalesced. This indicates that the different double-melting transitions of BPAPP observed in the DSC (Fig. 6) did not involve a change in the crystalline form. Thus, the low-temperature endothermic transition may be attributable to the disordering of 'non-perfect' BPAPP crystalline domains. The crystallinity calculated from patterns (b)–(e) in Fig. 3 was about 30%, and did not change with annealing temperature. Prolonged annealing (e.g. at 200 °C for 24 h) or stretching of the film (e.g. at 180 °C) to its 2.5-fold in length did not lead to higher crystallinity. The stretched samples did not show oriented diffraction, and hence the chain conformation could not be deduced.

The multiple melting behavior of several flexible, semicrystalline polymer systems has been studied and attributed to a variety of reasons including pre-existing multiple crystal structures and reorganization of previously less-ordered structures [13]. Polymers with rigid chains and exhibiting multiple melting behavior are hardly known, except for the semi-crystalline poly(ether ether ketone) (PEEK) that shows double melting transitions. Lee and Porter [14] attributed the low-temperature endotherm in the case of PEEK to the melting of 'non-perfect' original crystals and the high-temperature endotherm to the melting of crystals reorganized during the heating scan. In the case the thermal behavior of polypropylene fractions, Paukkeri and Lehtinen [15] also interpreted the higher melting peak as due to the reorganization of the less ordered domains of the crystalline material during the scan. They found that the second peak was absent for high molecular weight fractions, as well as for those with high isotactic content. The double melting is observed frequently with samples of low molecular weight, and wide distribution, or with head-to-head defects in the case of polymers such as PVF_2. The M_n and M_w for the samples investigated by Lee and Porter were 14,100 and 38,600, respectively. The molecular weight could not be determined for the present polymer.

BPAPP is semi-rigid in its backbone structure due to the presence of aromatic diimide and the piperazine moieties and have comparable chain mobility as PEEK [14], as evidenced by their similar T_g ($T_{g,PEEK} = 143$ °C; $T_{g,BPAPP} = 148$ °C). The double melting behavior of BPAPP can also be attributed to the reorganization process, similar to that in PEEK. Since the low-temperature transition of BPAPP shifted continuously to a higher temperature as the annealing temperature increased, it cannot be attributed to a real melting of the as-formed crystals but rather a partial disordering of weakly structured polymer chains. The high-temperature transition can be ascribed to the final melting of the reorganized polymer crystals.

Whether or not the PEEK and BPAPP can be considered to be similar in terms of flexibility (their T_g's being about the same as noted above), there is a striking parallel in the behavior of the double melting endotherms in the thermal analysis. Table 2 shows the effect of different heating rates (for the sample precipitated from chloroform solution and dried at 80 °C under vacuum), on the peak temperatures and the heats of fusion of the low- and high-temperature transitions (endo-1 and endo-2, respectively). As the heating rate increased, the heat of fusion of endo-1 remained basically unchanged but that of endo-2 decreased. The same decrease in heat of fusion of endo-2 was observed for PEEK [14], but an increase in heat of fusion of endo-1 was found. Lee and Porter [14] attributed this observation to the premise that as the heating rate was increased, the amount of crystalline region that has time to recrystallize decreased, leading to a smaller high temperature endotherm. However, in the BPAPP system, the reorganization of disordered structures may not take place rapidly at a low temperature (e.g. <180 °C) and therefore effect of the heating rate on heat of fusion of endo-1 can be expected to be minimal. As also noted by Lee and Porter, the total heat of fusion of both endotherms (ΔH_{1+2}) decreases with increasing rate. Table 2 shows that peak melting temperature corresponding to endo-1 increases, while that of endo-2 decreases with an increasing heating rate. This was again explained [14] on the basis of shorter reorganization times with an increase in heating rate. Thus the double melting behavior observed with BPAPP can be ascribed to the reorganization process invoked by other researchers, and not due to a crystalline polymorphic change.

To investigate the crystallization and melting behaviors of BPAPP further, temperature-modulated DSC (TMDSC) were carried out on the samples having different thermal histories. Fig. 7 displays the overlay of reversing (A) and non-reversing (B) TMDSC traces of the BPAPP samples (isolated from chloroform) that were dried under vacuum overnight at 80 °C (a), annealed for 2 h at 200 °C (b) and 240 °C (c), respectively, and heated to 300 °C and subsequently crystallized for 10 h at 200 °C (d) and 220 °C (e), respectively. All the reversing traces consist of a glass transition and a broad endothermic transition, while the non-reversing traces contain two endothermic transitions, corresponding to the low- and high-temperature melting transitions, and an enthalpy relaxation peak at T_g. By comparison, the broad endotherms in the reversing traces, regardless of the thermal history of samples, began at the onset temperature of endo-1 and covered the whole temperature range from endo-1 to endo-2. Therefore, both low- and high-temperature transitions of BPAPP should be considered as a reversible process, and a reversible partial disordering and reorganization process should exist between these two transitions.

Table 2
Peak temperatures (T_m) and heats of fusion (ΔH) of low- and high-temperature endothermic transitions (endo-1 and endo-2) of BPAPP at different heating rates

Heating rates (°C/min)	Endo-1		Endo-2		ΔH_{1+2} (J/g)
	T_m1 (°C)	ΔH_1[a] (J/g)	T_m2 (°C)	ΔH_2 (J/g)	
2	165	10.81	257	16.95	27.76
5	171	10.25	255	12.11	22.36
10	176	8.33	252	8.12	16.45
20	179	10.56	251	7.48	18.04
30	181	10.86	249	6.16	17.02

Notes: T_m1, T_m2 and ΔH_1, ΔH_2 represent the peak temperatures and heats of fusion of low- and high-temperature endotherms; ΔH_{1+2} is the total heat of fusion.
[a] Glass transition overlaps with low-temperature endotherm. The ΔH_1 values are for comparison only.

4. Conclusions

A unique crystallization and melting behaviors of a semicrystalline polyimide derived from BPDA and 1,4-bis(3-aminopropyl)piperazine are discussed. This polymer exhibits solubility in chloroform and dichloromethane, but not in other solvents that are commonly used for polyimides. This cannot be rationalized on the basis of solubility parameters alone, but perhaps attributed to weak halogen mediated interactions. While melt crystallization occurs in a narrow range of 200–220 °C after a long time (10 h), the samples precipitated from chloroform require annealing only for 2 h, at temperatures above the T_g. A double-melting behavior was observed for the sample isolated from its chloroform solution, as well as those crystallized from the melt. However, the heat of fusion was more pronounced with the former. A partial disordering—reorganization—final melting model, as was proposed for PEEK and other polymers, may account for the double-melting behavior of this polymer.

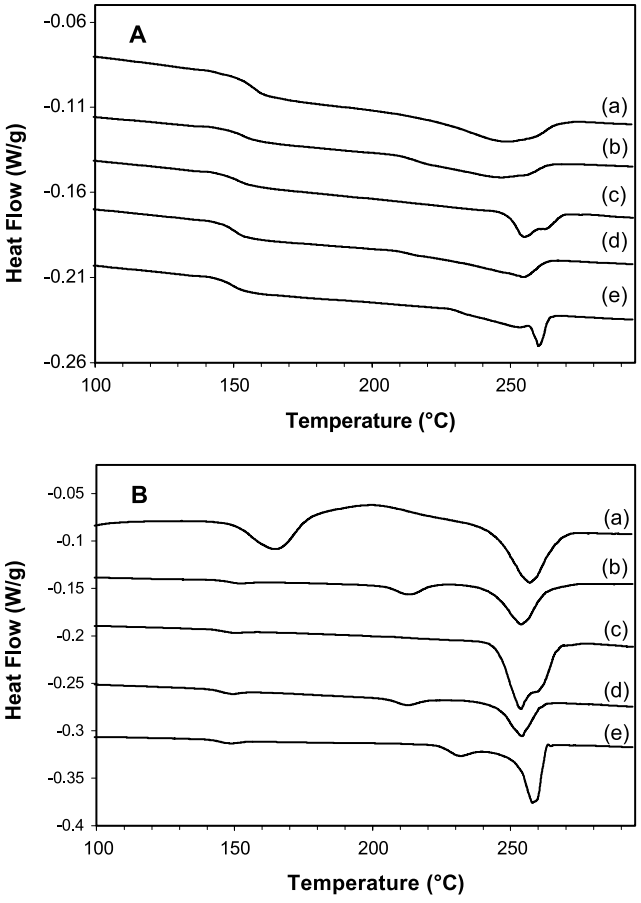

Fig. 7. TMDSC traces of BPAPP with different thermal histories, with a heating rate of 3 °C/min, modulation period of 60 s, and modulation amplitude of 1 °C. The reversing (A) and non-reversing (B) traces are shown for the samples that were (a) dried at 80 °C under vacuum (~1 mm Hg) overnight, thermally annealed for 2 h at (b) 200 °C and (c) 240 °C, respectively, heated to 300 °C and then crystallized for 10 h at (d) 200 °C and (e) 220 °C, respectively. The peaks are not normalized to the sample weight.

Acknowledgements

We thank the Natural Sciences and Engineering Research Council of Canada for financial support.

References

[1] (a) Tashiro K, Yoshioka A. Macromolecules 2002;35:410.
(b) Guerra G, Vincenzo V, Vitagliano M, De Rosa C, Petraccone V, Corradini P. Macromolecules 1990;23:1539.
(c) Ishihara N, Seimiya T, Kuramoto M, Uoi M. Macromolecules 1986;19:2465.
[2] (a) Chen M, Chao S-C. J Polym Sci Polym Phys 1998;36:2225.
(b) Lee Y, Porter RS. Polym Eng Sci 1986;26:633.
[3] (a) Kubo H, Okamoto M, Kotaka T. Polymer 1998;39:4827.
(b) Makarewicz PJ, Wilkes GL. J Polym Sci Polym Phys Ed 1978;16:1529.
[4] (a) Loos J, Schimanski T, Hofman J, Peijs T, Lemstra PJ. Polymer 2001;42:3827.
(b) Amornsakchai T, Cansfield DLM, Jawad SA, Pollard G, Ward IM. J Mater Sci 1993;28:1689.
(c) Sheehan WC, Cole TB. J Appl Polym Sci 1964;8:2359.
[5] Ghosh MK, Mittal KL. Polyimides: fundamentals and applications. New York: Marcel Dekker; 1996.
[6] Mittal KL. Polyimides and other high temperature polyimides: synthesis, characterization and applications. vol. 2. Zeist, Netherland: VSP BV; 2003.
[7] (a) Wang ZY, Qi Y. Macromolecules 1994;27:625.
(b) Fukai T, Yang JC, Kyu T, Cheng SZD, Lee SK, Hsu SLC, et al. Polymer 1992;33:3621.
(c) Su TM, Ball IJ, Conklin JA, Huang S-C, Larson RK, Nguyen SL, et al. Synth Met 1997;84:801.

[8] (a) Ratta V, Ayambem A, McGrath JE, Wilkes GL. Polymer 2001; 42:6173.
(b) Srinivas S, Caputo FE, Graham M, Gardner S, Davis RM, McGrath JE, et al. Macromolecules 1997;30:1012.
[9] Kricheldorf HR. Adv Polym Sci 1999;141:83.
[10] Song N, Wang ZY. Macromolecules 2003;36:5885.
[11] (a) Wang M, Braun H-G, Meyer E. Macromolecules 2004;37:437.
(b) Schönherr H, Frank CW. Macromolecules 2003;36:1188.
(c) Tauchi K, Miyaji H, Izumi K, Hoshino A, Miyamoto Y, Kokawa R. Polymer 2001;42:7443.
[12] (a) Desiraju GR, Steiner T. The weak hydrogen bond. Oxford: Oxford University Press; 1999.
(b) Corradi E, Meille SV, Messina MT, Metrangolo P, Resnati G. Angew Chem Int Ed 2000;39:1782.
(c) Abraham MH, Enomoto K, Clarke ED, Sexton G. J Org Chem 2002;67:4782.
(d) Anzellotti A, Briceno A, Delgado G, Diaz de Delgado G, Fontal B. Acta Crystallogr Sect C 2002;58:m355.
(e) Majumdar K, Majumder K, Lahiri SC. J Ind Chem Soc 2002;79: 811.
[13] (a) Caminiti R, Isopo A, Orru MA, Albertini VR. Chem Mater 2000; 12:369.
(b) Chang LL, Huang BS, Woo EM. Polymer 2001;42:8395.
(c) Marand H, Prasad A. Macromolecules 1992;25:1731.
(d) Sasaki T, Sunago H, Hoshikawa T. Polym Eng Sci 2003;43: 629.
(e) Moyses S, Spells SJ. Macromolecules 1999;32:2684.
(f) Chung JS, Cebe P. Polymer 1992;33:2312.
[14] Lee Y, Porter RS. Macromolecules 1987;20:1336.
[15] Paukkeri R, Lehtinen A. Polymer 1993;34:4083.